IN SITU MEASUREMENT OF THE SAMPLE TEMPERATURE IN THE BM29 CRYOSTAT III BY CU-K EXAFS

J. RÖHLER and D. LÖWEN
Fachgruppe Physik, Universität zu Köln

Abstract. From simultaneous transmission and total electron yield (TEY) measurements of the Cu-metal K EXAFS we find that their amplitudes at low T are dampened up to 25 % relative to the established transmission standard. All spectroscopic artefacts causing dampened EXAFS amplitudes are considered in detail and were found absent. We conclude that the "damping" is due to a thermal malfunction of the He cryostat ("Cryo III"). Using the correlated Debye-model the nominal temperatures from a thermometer at the sample platform are found to deviate up to 125 K from the actual temperature at the sample site.

1. Introduction

The commissioning run BLC 268 was dedicated to a comparative study of the EXAFS amplitudes obtained from the total electron yield (TEY) and the standard transmission detection. Transmission and TEY EXAFS exhibit a different background behavior, resulting in complications with respect to the normalisation of the EXAFS absorption coefficient $\mu(E)$. The transmission background follows the well-known decaying Victoreen-type form, reflecting the decreasing absorption coefficient with increasing x-ray energy. In contrast the TEY background increases monotonically throughout the whole spectrum due to the increase in the flux of emitted photoelectrons and secondary electrons with x-ray energy. We have recently developed a TEY detector head operational in a continous flow He cryostat between about 4 and 300 K. It uses the He exchange gas, coupling the sample thermally to the cold head of the cryostat, also for amplification of the TEY current. Using this detection technique it is important to understand the previously observed effects of the variable cryogenic temperatures on the background of the TEY signal. The generically positive slope of the TEY background is usually corrected for during background subtraction and/or data analysis. To good approximation the correction may be done by extrapolation of the pre-edge background to an appropriate steering point at the end of the spectrum. Temperature dependent data from simultaneous TEY and transmission measurements of the Cu-K EXAFS from elemental Cu will allow us to quantify the temperature effects on the TEY background.

Unfortunately we could not carry out this experimental program so far. Using the recently installed He cryostat "Cryo III" the amplitdes of our low T transmis-

sion EXAFS were found significantly dampened relative to the well established Cu metal standard. Here we show that the dampened amplitudes are due to a thermal malfunction of the Cryo III. Spectroscopic artefacts could be as well at the origin of the damping. Therefore we have carefully checked all non thermal sources able to cause the distorted EXAFS amplitudes in our measurement. This check is outlined in section 2. In section 3 we determine the actual temperatures at the sample site from a full multiple scattering analysis of the low T EXAFS and compare them with the nominal temperatures. The simultaneously measured TEY spectra will be reported and discussed in a forthcoming paper.

2. Experimental

The K EXAFS of elemental Cu were simultaneously measured in the transmission and TEY modes, nominally between 25 K and 300 K. To do the first thing we checked the amplitudes of our transmission spectra against the well established standard data. For $T = 10 - 300$ K these are available from many sources, for example the EXAFS data archive, or as part of the FEFF software package (1). Precision data between 10 K and 500 K have been recently published by Fornasini *et al.* (3).

2.1. SPECTROSCOPIC DETAILS

We have used a laminated, light tight foil of elemental Cu (BM 29 standard absorber, $d \simeq 10$ μm). It covered completely the rounded transmission window ($\simeq 2 \times 7\text{mm}^2$) and was fixed with adhesive Al tape on the sample plate. Silver paste at the edges of the Al tape and the sample plate bridged the insulating adhesive coating of the Al tape. Thus the lower side of the foil was put in good contact with the electrical ground of the TEY detector. A well defined electrical grounding of the detector was secured by electrical (and thus also thermal) insulation of the TEY sample plate from the platform at the lower end of the rod. An insulated needle-like electrode served as collector of the TEY.

The storage ring was operated in the hybrid mode with typically 185 mA. The vertical gap of the entrance slits was set to 0.3 mm, and the horizontal collimation to 5 mm using the experimental slits. The acquisition time was 2 s/point. We find perfect coincidence between our transmission and the archived standard spectra at 300 K (Figs. 1 and 2), but not at low T (Figs. 3 and 4). At 25 K the average amplitude of the EXAFS absorption coefficient $\chi(k)$ is found dampened by about 25 % relative to that of the standard at 10 K. Note that our 25 K spectrum and the 10 K standard are comparable since for $T \leq 30$ K only zero point fluctuations contribute to the EXAFS amplitudes. This is clearly seen in Fig. 5 exhibiting the standard spectra between 10 and 300 K.

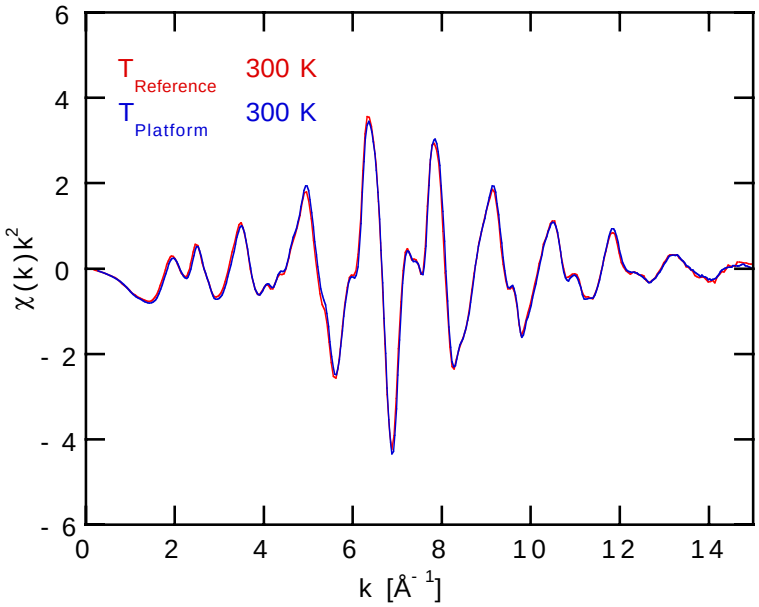

Figure 1. Cu-K EXAFS, χk^2, of elemental Cu metal measured in the transmission mode. *Blue* : 300 K, this work. *Red* : 300 K (red), reference data of Newville *et al.* (1)

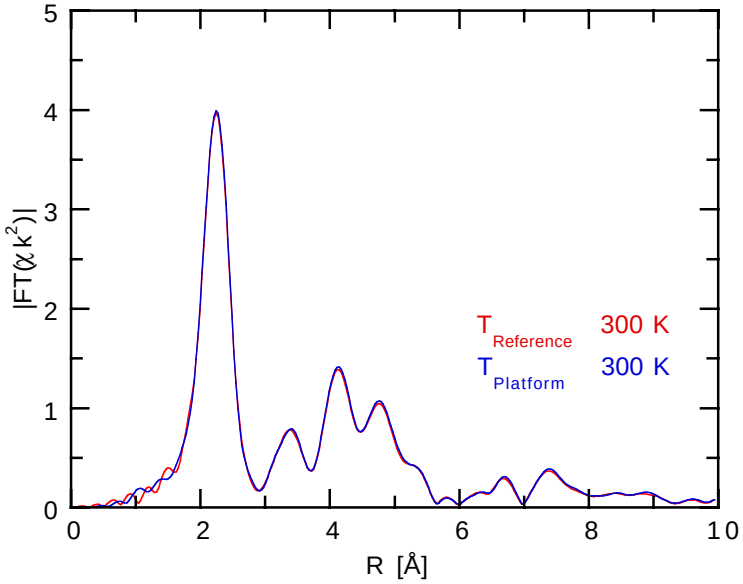

Figure 2. Moduli of the Fourier transforms, $|\mathrm{FT}(\chi k^2)|$, as obtained from the data in *Fig. 1* using a Hanning window $k = 2 - 15$ Å^{-1}.

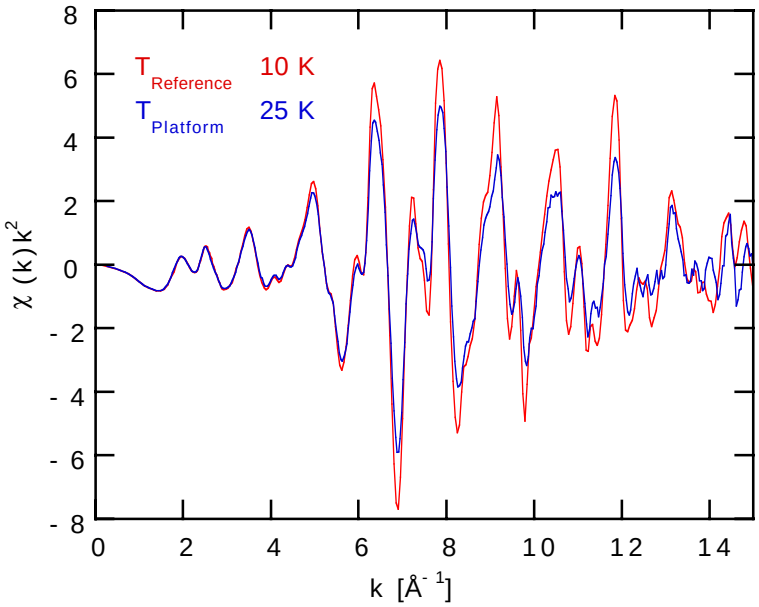

Figure 3. Cu-K EXAFS, χk^2, of elemental Cu metal measured in the transmission mode. *Blue* : 25 K (nominal), this work. *Red* : 10 K (red) standard data of Newville *et al.* (1)

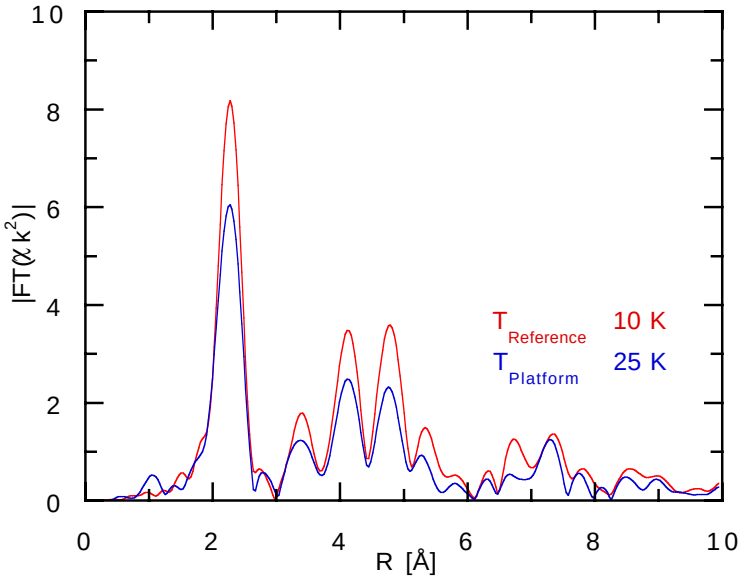

Figure 4. Moduli of the Fourier transforms, $|\mathrm{FT}(\chi k^2)|$, as obtained from the data in *Fig. 3* using a Hanning window $k = 2 - 15$ Å^{-1}.

The perfect coincidence of our 300 K spectra with the standard indicates the absence of distorting experimental artefacts around 300 K, however not necessarily at low T. Here various spectroscopic errors may be at the origin of the damping: instable detectors, drifting detector offsets, temperature induced "leakage" effects due to filtered higher harmonics, pin holes or sample inhomogeneities, and "cutting" misalignments of the sample. In the following we discuss these effects in detail.

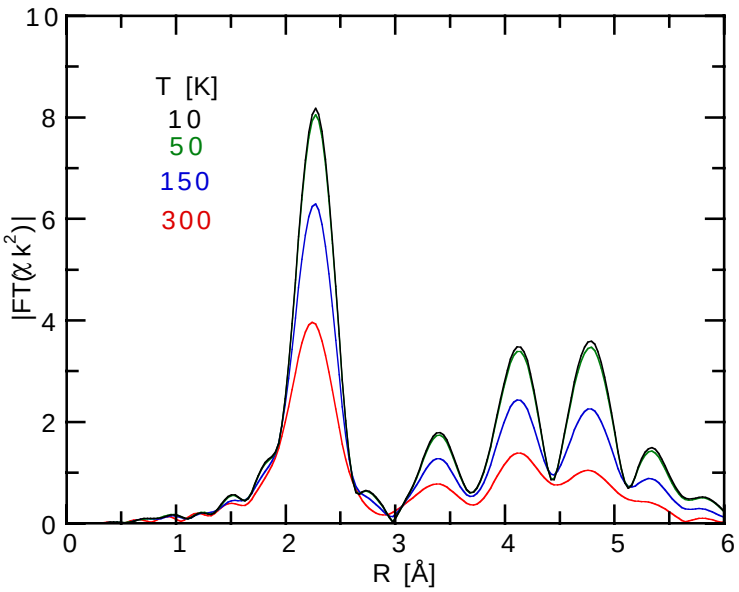

Figure 5. Cu metal standard EXAFS of Newville *et al.* (1): Moduli of the Fourier transforms, $|\mathrm{FT}(\chi k^2)|$, between 10 K and 300 K.

2.1.1. *Linearity and Offset*
For the detection we have used sealed ionization chambers filled with 260 mbar Ar (+ He) for the measurement of I, and with 100 mbar Ar (+He) for I_0. Both chambers were operated with 600 V guaranteeing linear detection for the typical photon flux from the bending magnet. The gas pressures were found constant during the whole run. Time dependent distortive effects from the detectors can be therefore excluded. The offsets caused by the dark current and the electrometers were automatically compensated.

2.1.2. *Higher harmonics*
The white beam delivered from the bending magnet 29 was monochromatized with a double crystal monochromator of the fixed exit type. We used a pair of He cooled Si [111] crystals. Due to the crystalline symmetry of the diamond structure the Bragg condition is fullfilled for the [111], [333], reflection planes, but not for the [222]. Thus the 1. higher harmonics around 18 keV was naturally suppressed, but not the 2. around 27 keV, and all allowed of higher order. We have moved the plane mirror device into the monochromatized beam to create a low energy bandpass cutting at $E \simeq 11$ keV, the upper limit of our Cu-K edge scans. The corresponding reflection angle of the mirror was 2.5 mrad. In addition we operated the double crystal monochromator in the detuned mode therewith exploiting the significantly different reflection widths of the fundamental and the higher harmonics for the suppression of the latter. With a detuning parameter of 0.5 we estimate the effective content of higher harmonics after the mirrors to be $\leq 10^{-6}$. Since we have used a spectroscopically thick Cu foil (optimized for the best statistical signal from an absorption step of $\Delta\mu d \simeq 2.4$), the experiment was highly sensitive to distortions

from a even weakly spectrally contaminated beam. To be less sensitive to the higher harmonics one usually optimizes the absorber thickness for an absorption step of $\Delta\mu d \leq 1$. Despite of the unfavorably thick absorber we have measured at 300 K the correct amplitudes (Figs. 1, 2), confirming the very efficient suppression of the higher harmonics.

Assuming that at low T the beam has possibly hit inhomogenous or porous areas of the sample foil, or moved into blank areas of the transmission window, the dampened amplitudes of $\chi(k)$ could be attributed to not attenuated fractions of the beam (leakage). Hence the true absorption $\mu(E)d$ would be significantly distorted :

$$\mu'(E)d = ln\left(\frac{I_0(E)}{I(E)} + \alpha(E)\right)$$

Here $I(E)$ are the incoming, $I_0(E)$ the transmitted intensities of the true absorption, and $\alpha(E)$ the leakage, "shunting" the true absorption. Since leakage, of whatever origin, affects the total absorption, it is easily discovered in the not normalized raw spectra from a reduced height of the absorption step. Fig. 6 displays the step heights as a function of temperature. They are are found constant within $\pm 0.6\%$, which definitely excludes leakage is a the origin of the dampened low T $\chi(k)$. The step height of the 160 K spectrum falls apart from one standard deviation. This spectrum was measured subsequently a new injection. Obviously the monochromator drifted during the scan still towards the thermal equilibrium and thus distorted the spectrum.

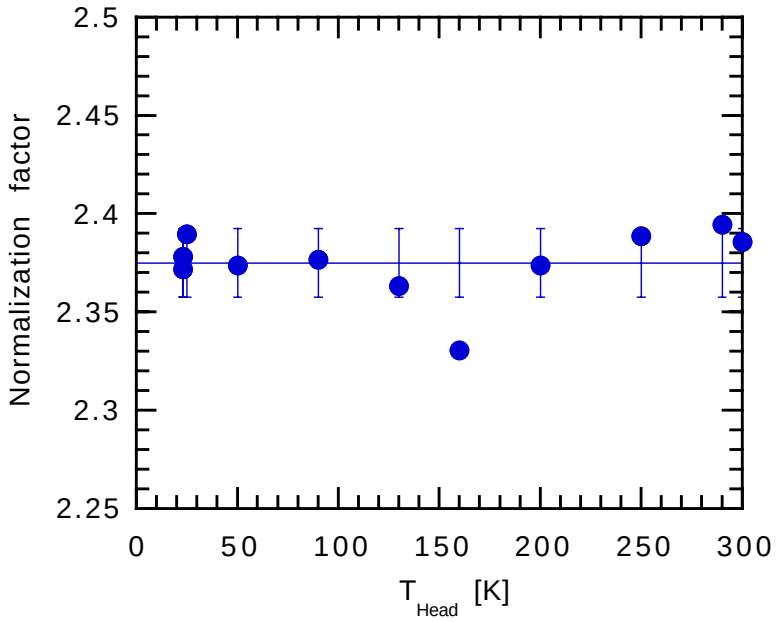

Figure 6. Normalization factors as a function of temperature. The error bars indicate one standard deviation. The 160 K point was recorded directly after a new injection.

2.2. MISALIGNEMENT

At low T the beam hits the absorber at positions vertically shifted relative to that at room temperature. This effect is due to the thermal contraction of the sample rod according to $\Delta L = L_0 \Delta T \alpha$. Here α is the thermal expansion coefficient of the rod, ΔT the temperature gradient, L_0 the thermally effective length of the rod, and ΔL the change of the length. The thermal expansion of the TEY sample rod had been measured in a previous run using Cryo II (manufacturer Oxford). Its expansion with temperature relative to $T \simeq 0$ is shown in Fig. 7. It amounts to $\simeq 0.4$ mm from 0 to 300 K, that is comparable to the vertical width of the beam, and 1/5 of the vertical width of the transmission window.

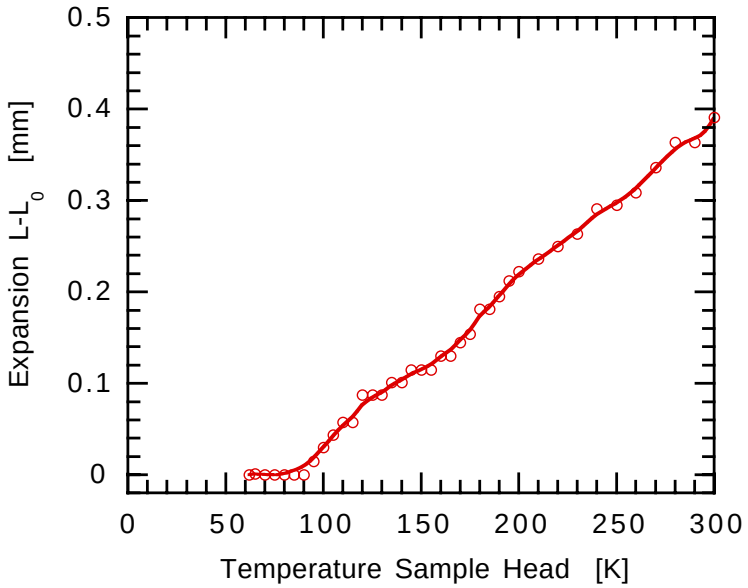

Figure 7. Relative thermal expansion of the unmodified sample rod as determined in Cryo II (Oxford)

Hence the beam probes different sample areas at different T. If, as discussed in the previous subsection, the sample is uniform and the measurement free of leakage, sampling of different sample areas will not distort the amplitudes. But if an opaque object, such as an edge of the transmission window, moves into the beam therewith cutting a fraction of it, the absorption μd will be offset.

$$\mu d = ln \frac{I_0(E)}{I(E)\epsilon}$$

Here ϵ is the cut fraction of the beam area. Clearly, this is a *linear* effect, not affecting the height of the absorption step, and not damping the amplitude of $\chi(E)$. However it deterioates the signal to noise ratio (S/N). Any tiny positional fluctuation of the incoming beam changes the effective area of the absorber, and thus modulates the absorption coefficient. Glitchies and other systematic distortions are no longer cancelled, because the parasitic components in the monochromatic beam are cut

as well and no longer compensated through the ratio of $I_0(E)$ with $I(E)$. And if the beam position drifts with increasing energy, the slope of the background will be affected, too. This "cutting" type of misalignement is easily seen in the raw data: the absorption is offset, the height of the absoroption step stays unaltered, but the S/N is significantly deterioated.

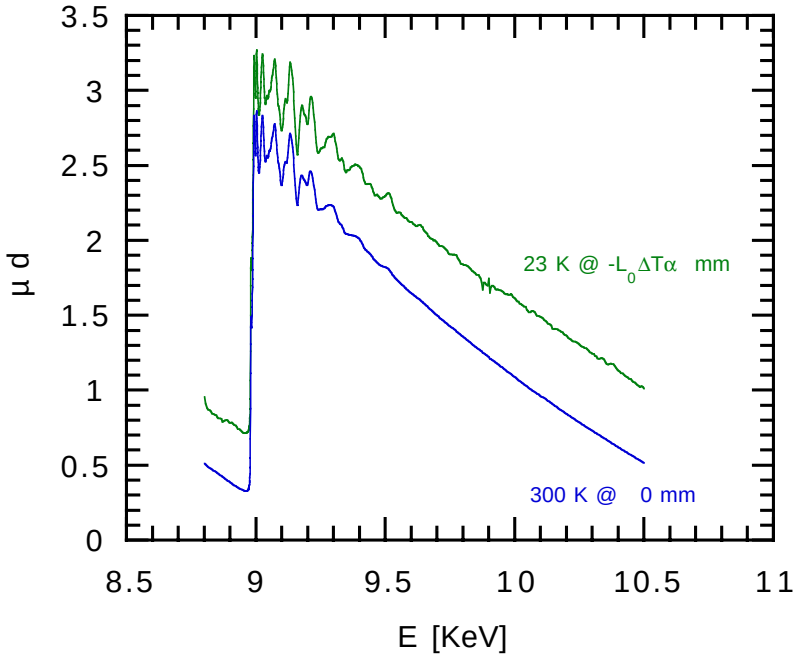

Figure 8. Cu K absorption at 300 K (blue) and "23 K" (green), offset due to the thermally driven vertical sample displacement cutting the beam. Note the unchanged height of the absorption step, and the deterioated S/N.

Fig. 8 displays the Cu K absorption at 300 K (blue) and at "23 K" (green). The low T" spectrum is offset by $\delta\mu d \simeq +0.4$ indicating that about 50 % of the sample area is cut from the transmission. The S/N ratio is deterioated, and the glitchie around 9.9 KeV significantly enhanced. But the height of the absorption step stays unaltered, confirming the very effective suppression of the higher harmonics. Fig. 9 displays some spectra of the temperature cycle: 300 K (blue) → "23 K" (green) → 290 K (black). We find a hysteresis of the offset, most probably due to a different thermal overall state of the cryostat after cycling. The temperature of the coldhead, $T_{coldhead}$, was 87 K at the beginning, and 47 K at the end of the cycle. Subseqent to the cycle we have *isothermally* changed the vertical sample position, nominally by -0.2 mm, therewith deliberately moving the lower edge of the transmission window into the beam. The offset of this 300 K (red) spectrum is found identical with that of the thermally displaced "23 K" (green) spectrum ! Notably the two step heights coincide, as well as the background and noise patterns due to the "cutting effect". And not unexpected the amplitudes of the isothermally displaced 300 K (red) spectrum coincide with the standard data of Newville *et al.* (1), see Fig. 10,

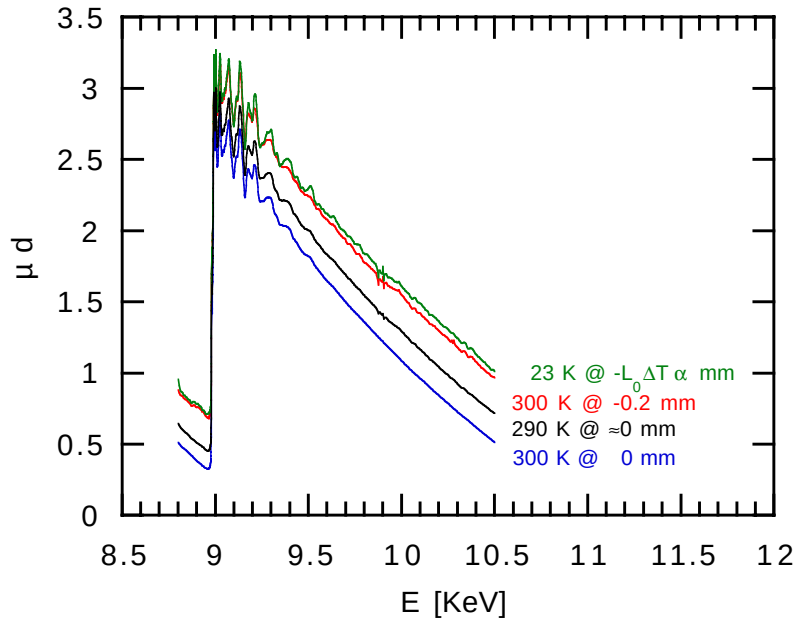

Figure 9. Cu-K absorption ofrom the temperature cycle: 300 K (blue) → "23 K" (green) → 290 K (black). Offset due to the thermally driven vertical sample displacement cutting the beam. Red : 300 K *isothermally* displaced by −0.2 mm. Note the coinciding step heights, background and noise patterns of the green "23 K" and the isothermally displaced red 300 K spectra.

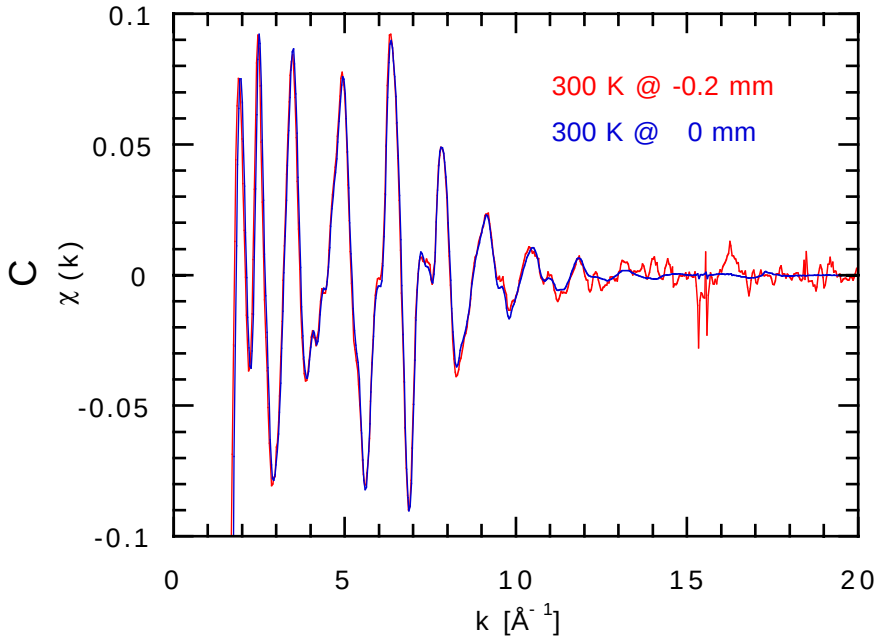

Figure 10. $\chi(k)$ at 300 K from the aligned position 0 mm (blue), and a misaligned position (red). The misalignment is −0.2 mm relative to the position of "23 K" spectrum (green) in Figs. 8 and 9. Note the absence of damping effects. The bad S/N restricts the usefull data range to $k \leq 15$ Å^{-1}, which was used throughout the whole data analysis.

and our at 300 K (Fig. 1). And, as expected the spectrum is deterioated by enhanced systematic noise limiting the usefull data range to $E \leq 9.85$ KeV or $k \leq 15$ Å^{-1}.

2.3. CRYOGENIC DETAILS

The transmission K EXAFS of elemental Cu are *the* experimental standard for the spectroscopic quality of x-ray absorption measurements in the energy range around 9 KeV. Its T dependence has been analyzed with high accuracy, too. Good agreement of its thermal behavior with lattice models is already found using the simplifying Einstein ansatz, or the more elaborate correlated Debye ansatz (2), and with thermal expansion data (3). The low T regime between 10 and 300 K is well described by $\Theta_D = 317$ K, in good agreement with the tabulated number of 320 K. Here Θ_D is the Debye temperature. Hence the T dependent EXAFS data of elemental Cu may be used as an *in situ* thermometer, either simply by measurements of the nearest neighbor Debye-Waller factor, $\sigma^2_{nn}(T)$, or more elaborately by multiple scattering fits to the correlated Debye model.

The TEY sample rod (modified Oxford model) was operated in the sample tube of the He cryostat Cryo III. Therein cooling of the sample is achieved by static He exchange gas transporting the heat of the sample towards the heat sink at the bottom plate connected with the cold head. A calibrated Lake Shore Si diode inserted in a hole of the sample platform (containing also the resistive heaters) was used for the remote controlled temperature settings ($T_{platform}$) and served also as thermometer for the nominal temperature at the sample site. The position of the sample site was about 17.4 mm below the sample platform, and 32.3 mm above the heat sink at the bottom of the sample tube (in vertical direction). Due to the exchange gas cooling the temperature gradient between the sample site and the sample platform was expected to be negligably small, and to have a *positive* sign. A second thermometer

TABLE I. Thermal parameters of the low temperature run, see also the text.

$file$: cu_#.dat	$T_{platform}$ [K]	p_{tube} [mbar]	$T_{coldhead}$ [K]	p_{pump} [mbar]	P_{medium} [%]
28	300	127	87	?	?
29	26	64	3.2	50	0
31	23	125	10	14	0
33	50	145	10	14	?
34	90	174	13	14	31
35	130	190	11	14	52
36	160	213	12	14	68
37	200	237	14	13	87
38	250	260	41	5	63
39	290	276	47	5	72

probed the temperature at the cold head ($T_{platform}$) located about 150 mm below the sample site.

Table I lists the thermal parameters of the run. Cooling of the warm cryostat down to $T_{platform} = 25$ K was achieved within about 3 h. Upon heating the sample platform in steps of about 40 K ($T_{platform} > 25$ K) the temperatures reached the set point within a few minutes and got stable within ≤ 0.1 K.

3. Results and data analysis

Useful data were obtained up to $k = 15$ Å^{-1}, and normalized using AUTOBK. To do the first thing we verified the standard fits (using 12 paths and $R_{max} = 5.1$ Å) to the low T reference data (1).

The three data-set fit (10, 50, 150 K) using FEFFIT and its built-in Debye function yielded $\Theta_D = 326$ K. This number is slightly larger than reported previously (2), probably due to our use of a shortened k-range $2-15$ Å^{-1} to be compared with $k = 2-19$ Å^{-1} in the standard fits.

Fig. 5 exhibits the Fourier transform spectra of the archived reference data at different temperatures from 10 K – 300 K, Fig. 11 the fit of the correlated Debye-Model to the 10 K spectrum. All fits were carried out in real space within $R = 1.75-3.25$ Å. $S_0^2 = 0.9061$ found from these fits was used as fixed parameter throughout the whole data analysis.

The Fourier transform spectra of our low-T measurements (nominally $25-300$ K are shown in Fig. 12, and Fig. 13 displays the 300 K measurement (blue) together with the fit (red). The fits to all low-T measurements are displayed in Fig. 14.

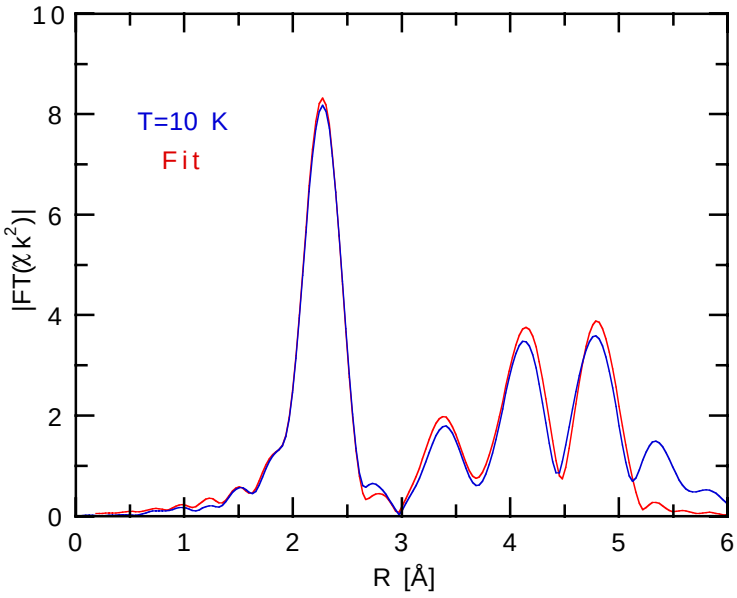

Figure 11. The three data-set fit (10, 50, 150 K) fit (red) to the 10 K Cu metal standard data (blue) of *Fig. 5* using the correlated Debye model, see text.

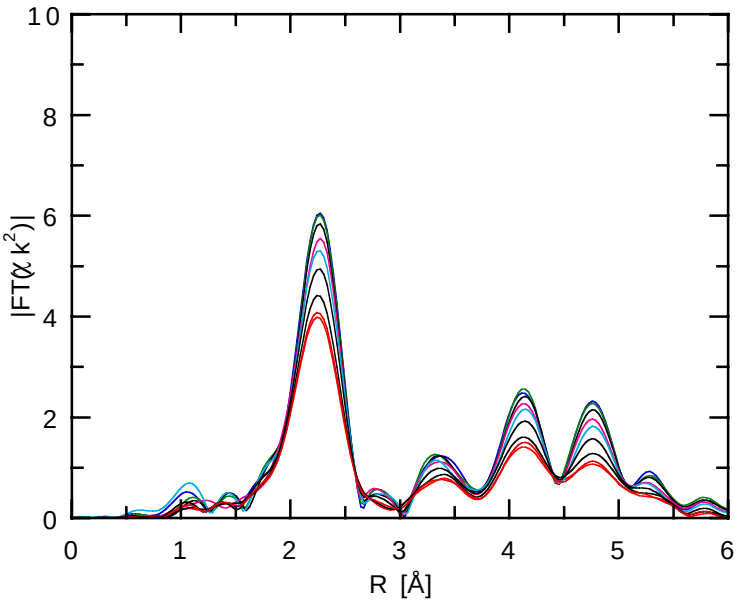

Figure 12. Fourier transform spectra, $|\mathrm{FT}(\chi k^2)|$, of elemental Cu obtained with the cryogenic parameters listed in Table I. The nominal temperatures determined at the sample platform range from 25 K to 300 K.

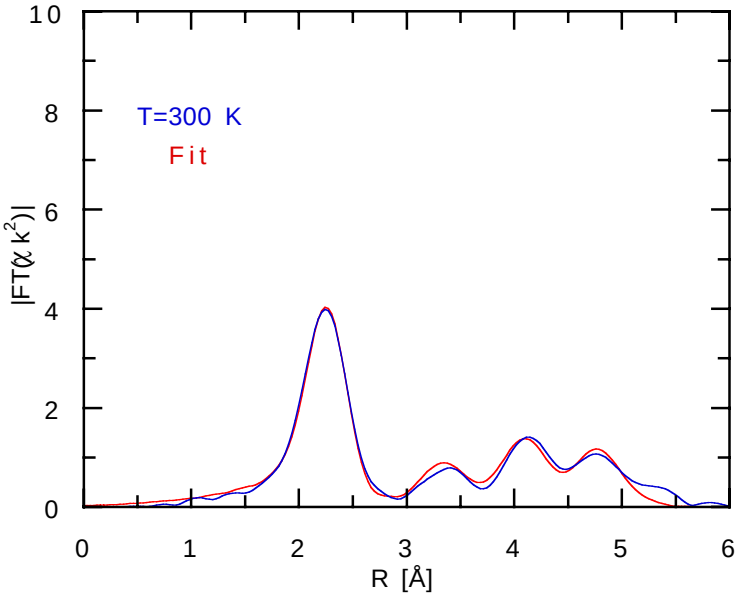

Figure 13. Fit (red) to the 300 K Cu metal data (blue, #28 in Table I) displayed in Fig. 12 using the correlated Debye model, see text. The fit matches also the 300 K reference spectrum co-plotted in Fig. 2.

Fig. 15 summarizes the temperature dependences of the Debye-Wallers factors σ^2_{nn} from fits without the correlated Debye model. The large discrepancy between our measurement and the reference data at low T is clearly visible. We find *e.g.* the nominal temperature of 25 K to correspond to the *in situ* temperature of about

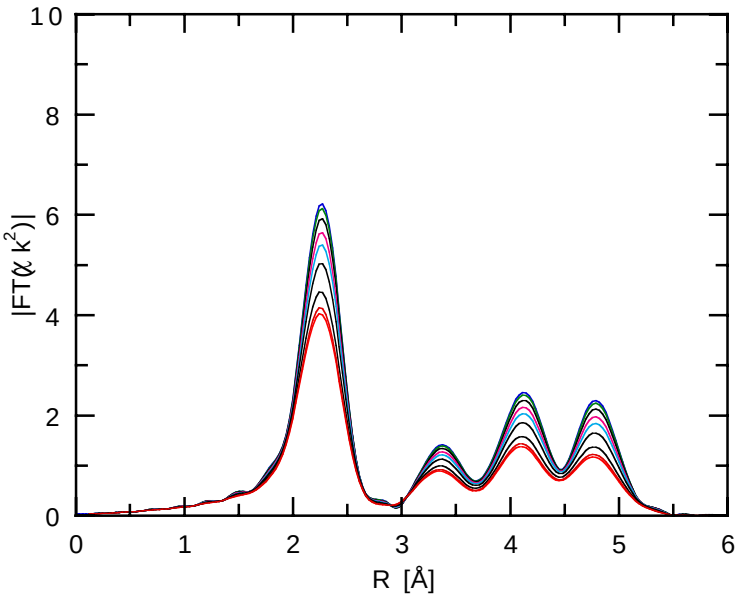

Figure 14. Fits to all Fourier transform spectra displayed in Fig. 12 using the correlated Debye model, see text.

155 K.

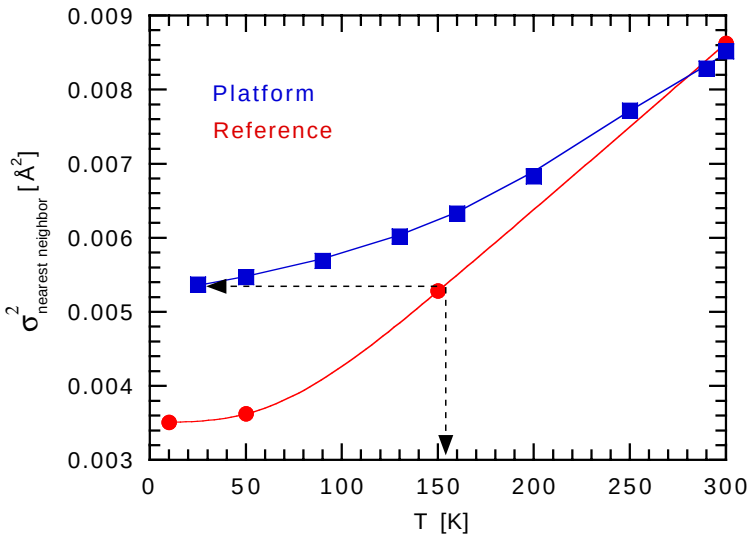

Figure 15. Debye-Waller factors, σ^2, of the *nn* pairs as a function of temperature. Red circles: reference data. Blue squares: our measurements plotted *vs.* the nominal temperatures. Drawn out lines connecting the data points are guides to the eye. The lowest temperature of our measurement turns out to be only about 155 K, not 25 K (arrows).

Applying the correlated Debye model to the analysis of our measurements we have used $\Theta_D = 326$ K as input (from the fits to the archived reference data). We thus obtained the actual *in situ* temperatures from our data. Plotting the Debye-Wallers factors σ^2 (triangles in Fig. 16) *vs.* these *in situ*temperatures we obtain a

Debye behavior in agreement with the reference data. Fig. 17 exhibits the deviation of the *in situ* temperature from the nominal temperature.

4. Discussion

We have shown that the dampened EXAFS amplitudes in our low T data have to be sought in a malfunction of the cryostat, cooling the sample site to only 150 K while the sample platform is at 25 K. Notably the strong temperature gradient between the sample site and the sample platform has a *negative* sign. Although closer to the heat sink, the sample site is found significantly warmer than the more distant sample platform. This could be simply due to wrong temperature readings, but the calibrated Lake Shore Si diode can be safely assumed to have operated correctly.

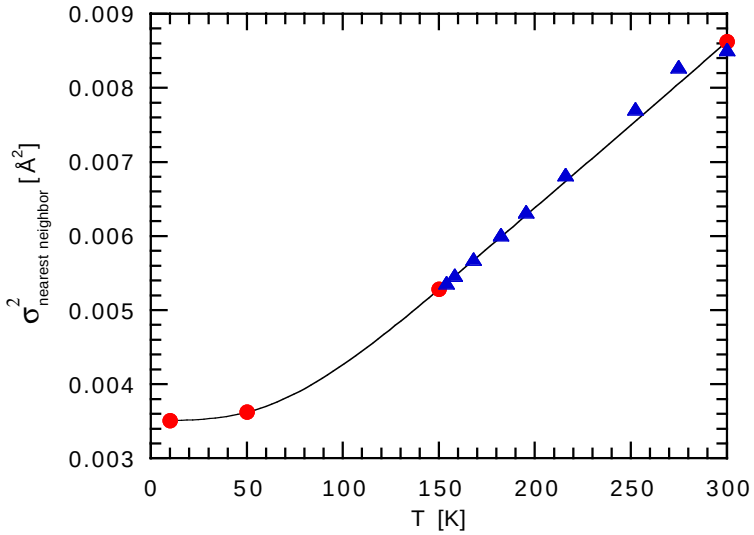

Figure 16. Fits of the correlated Debye model to the reference data (red circles) give $\Theta_D = 326$ K. Fits to the temperature dependent data of this measurement using this number yield their true temperature (blue triangles).

The pressure of the exchange gas environment ($p_{tube,300\ K} \geq 64$ mbar, measured at room temperature) was sufficiently high for its heat conduction to be independent on pressure: $\dot{Q} \propto N_{He}/\Lambda$. Here $\dot{Q}$ is the heat current, N_{He} the number of helium atoms per unit volume, and Λ their mean free path. Increasing pressure will increase n_{He} but equally decrease Λ. Thus the heat conduction of the dense gas is almost pressure independent. Pressure dependence however occurs at low densities where $\Lambda > d$ (Knudsen regime). Here d are the geometrical dimensions of the vessel, typically 50 mm. The corresponding He pressure for $\Lambda \geq 50$ mm is $p_c \leq 1.5 \times 10^{-3}$ mbar at 4 K. $p_{tube,300\ K} = 64$ mbar corresponds to a reduced pressure at He temperatures: $p_{tube,4\ K} = 4/300 \times 64 \simeq 0.85$ mbar $>> p_c$. Thus the sample site is equally well thermally coupled to the exchange gas at all temperatures.

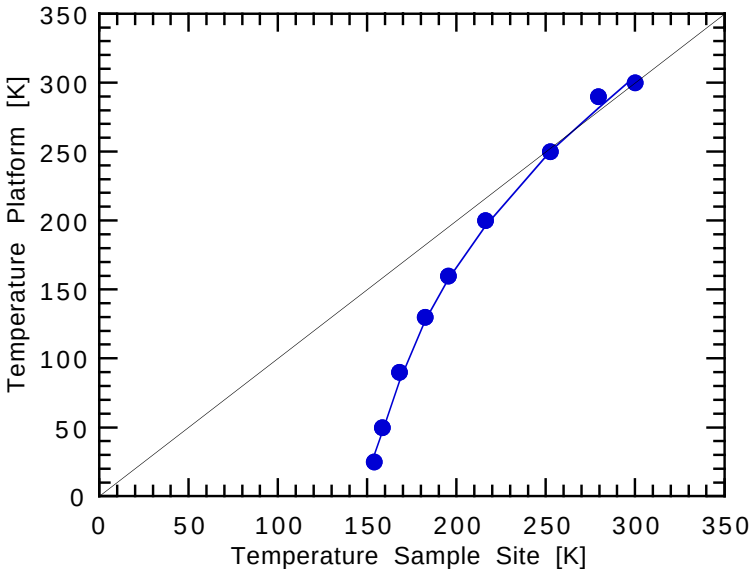

Figure 17. Temperature read from the Si-diode in the sample platform *vs.* the true temperature at the sample site as determined from the EXAFS Debye-Waller factors. Black diagonal: ideal thermal equilibrium between sample site and sample platform.

The local negative temperature gradient is most likely caused by a thermal shunt between the sample site and an only locally effective heat source. Local heating by the weak 50 pA ionisation current of the TEY detector can be safely discarded. But the sample area may be thermally shunted by the thermal radiation flowing onto the sample environment through the four especially large and thermally unscreened optical windows of ordinary Kapton foil. The clearance of these also thermally transparent x-ray windows was choosen so large that the heating of the exchange gas may be locally constrained to the sample site. Screening by the colder sample tube is not effctive because of the large windows. On the other hand side the sample platform beyond the sample site is completely screened by the closed sample tube. Thus the He exchange at the sample platform may adapt lower temperatures than the locally heated sample site, although the former is more distant from the heat sink at the bottom of the sample tube.

Acknowledgements

D.L. is grateful for the financial support by the ESRF allowing him to participate at the commissioning experiment of the TEY detector at BM29 (BLC 2685).

References

1. M. Newville, B. Ravel, and Y. Zhang (1992), NSLS beamline X-11A
2. M. Newville, M. (1995), Manual FEFFIT
3. P. Fornasini, S. a Beccara, G. Dalba, R. Grisenti, A. Sanson, M. Vaccari, and F. Rocca, Phys. Rev.**70** (2004) 174301.